

BIOPHYSICS OF RADIOFREQUENCY ABLATION

Dieter Haemmerich^{1,2}

¹Department of Pediatrics, Medical University of South Carolina, Charleston, South Carolina, USA; ²Department of Bioengineering, Clemson University, Clemson, South Carolina, USA

ABSTRACT: Radiofrequency (RF) ablation is a treatment modality that kills unwanted tissue by heat. Starting with cardiac arrhythmia treatment in the 1980s, RF ablation has found clinical application in a number of diseases, and is now the treatment of choice for certain types of cardiac arrhythmia, and certain cancers. During RF ablation, an electrode is inserted into, or steered intravascularly to the target tissue region under medical imaging guidance. Then, a tissue volume surrounding the electrode is destroyed by heating via RF electric current. This paper reviews the biophysics of tissue heating during RF ablation. Effects of electrical tissue conductivity and its change with temperature are discussed. Procedures and devices specific for cancer treatment, and for arrhythmia treatment are presented with brief discussion of additional clinical applications.

I. BACKGROUND

Radiofrequency (RF) ablation uses electric current to locally heat, and kill tissue. It is clinically used to treat various diseases including cancer, cardiac arrhythmia, varicose veins, and uterine bleeding¹⁻⁵. In this article we will discuss the biophysics of RF ablation in general, and in particular related to cardiac arrhythmia and cancer treatment since these are the two diseases where it is used most widely. In general, RF ablation is an image-guided procedure where medical imaging (e.g. CT, ultrasound, MRI) is used to guide an RF electrode to a target location (Fig. 1). Application of electric current in the radiofrequency range results in local tissue heating around the electrode, and subsequent tissue death due to protein coagulation. The main reason that RF ablation devices operate in the radiofrequency range (typically 450 – 500 kHz) is, that electrosurgical devices - which served as predicate - use this frequency range making regulatory approval for RF ablation devices easier. However, application of electric current of any frequency will result in tissue heating, but - depending on frequency of the current - other effects like chemical reactions (for DC current) and stimulation of tissue (at current frequencies below ~10 kHz) may occur in addition to the generation of heat.

Figure 1 shows a general setup, where an RF electrode is inserted into a target tissue volume (i.e. tissue to be destroyed). Application of electric current between the RF electrode and a reference electrode (ground pad) results in tissue heating around the RF electrode. The RF electrode is typically made of metal, and stainless steel, platinum, or Ni-Ti alloys are often used. Parts of the RF electrode may be electrically insulated to avoid heat generation of these insulated regions since tissue heating occurs only where the electrode is in direct contact with tissue. The skin below the ground pad will also heat up, but due to the large pad surface area temperature rises will be low. However, skin burns are one of the possible complications, particularly for tumor ablation procedures where high power is used for prolonged time periods

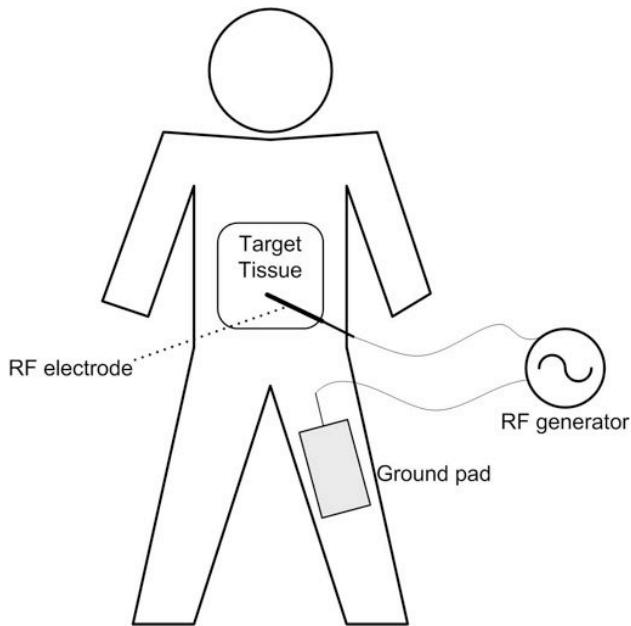


Figure 1. Overview of an RF ablation procedure. A RF electrode is inserted into the target tissue under imaging guidance. RF energy provided by a generator is applied to the electrode, and results in tissue heating around the electrode. A ground pad placed on the patient's thighs or back serves as return path for the RF current. Reproduced by permission from Editors (Shahram Vaezy and Vesna Zderic), *Image-guided Therapy Systems*, Norwood, MA: Artech House, Inc., 2009. © 2009 by Artech House, Inc.

II. THERMODYNAMICS OF RADIOFREQUENCY TISSUE HEATING

While inside the RF generator, cables, and RF electrode, free electrons serve as charge carriers, inside tissue ions (Na^+ , K^+ , Cl^-) carry the electric current. Application of electric current results in ion movement, and generation of heat due to friction (i.e. electrically resistive heating) (Fig. 2).

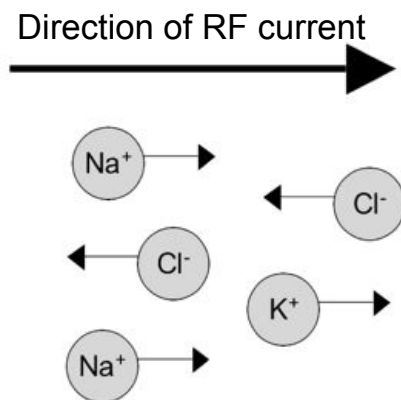


Figure 2. Electric current inside tissue is carried by ions. Ion oscillations due to applied RF current results in resistive tissue heating. For a typical frequency of 500 kHz, the direction of the current (and ion movement) changes a million times per second.

The amount of thermal energy generated locally by thermal ablation procedures in general is often quantified via the Specific Absorption Rate (SAR [W/kg]). For RF ablation, the local SAR is dependent on local electrical tissue conductivity and magnitude of local electric current density generated around the electrode (Equ. 1).

$$SAR = \frac{\sigma}{\rho} |E|^2 = \frac{1}{\sigma \cdot \rho} |J|^2 \quad (1)$$

σ ... tissue electrical conductivity

ρ ... tissue mass density

E ... electric field strength

J ... electric current density

Since in general the electric current density (and accordingly electric field strength) is only sufficiently high to cause significant direct heating very close to the electrode, thermal conduction contributes considerably towards the tissue heating at distances further from the electrode⁷. The heat transfer problem during RF ablation as well as other ablation methods can be mathematically described by the following heat transfer equation where T represents spatially and temporally varying tissue temperature⁸:

$$\rho c \frac{\partial T}{\partial t} = \nabla \cdot k \nabla T + \frac{E^2}{\sigma} - Q_{perf} \quad (2)$$

k ... tissue thermal conductivity

c ... tissue specific heat

T ... tissue temperature

The left-hand side term describes change in tissue temperature due to heating or cooling, and the first term on the right-hand side describes thermal conduction. The term Q_{perf} represents losses due to tissue cooling by blood perfusion. Mathematically several ways have been proposed to model this perfusion loss⁹ (see also paper by Payne et al. in this issue), but the most widely used model employs a distributed heat sink and was first proposed by Pennes more than 50 years ago¹⁰, and is applied to small vessels (< 1 mm). Larger vessels have to be included via other ways, e.g. by explicitly including these vessels in the model geometry.

Whether cell death occurs resulting from tissue heating depends on both temperature and time (see paper by Pearce in this issue). As a rough guideline, it takes a few minutes to kill cells at 50 °C, but only seconds at temperatures above 60 °C¹¹. Since thermal ablation procedures happen in a time frame of several minutes, the 50 °C isotherm is frequently used to approximate the ablation zone boundary¹². Figure 3 shows a typical tissue temperature profile at the end of a RF ablation with a tumor ablation electrode.

Target temperatures during RF ablation are in the range of 50 – 110 °C; higher temperatures are not possible as tissue begins to vaporize, and the electrically insulating vapor prevents any further RF energy deposition. At very high RF energy densities (typically close to the electrode),

carbonized tissue can form (often referred to as ‘tissue charring’); charring is an irreversible process and also limits further RF energy deposition. Therefore, applied energy has to be controlled to keep tissue temperature in the desired range and limit both vaporization and charring.

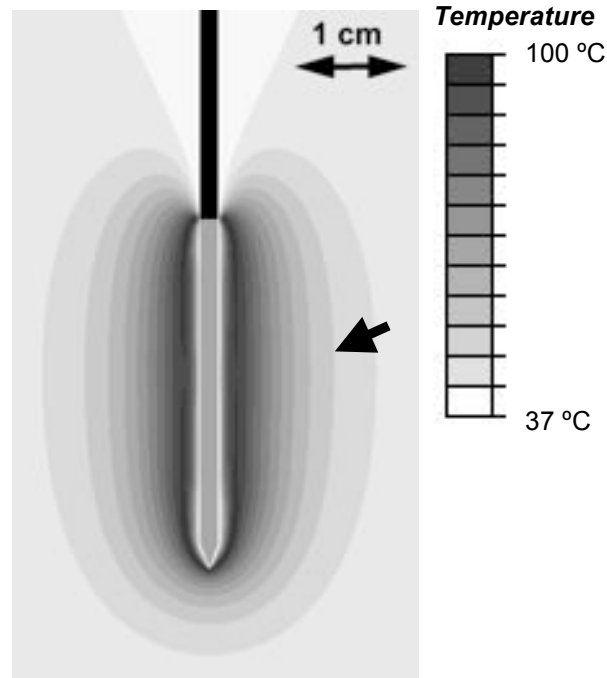


Figure 3. Tissue temperature profile at the end of a 12 min RF ablation with a cooled needle electrode (same as in Fig. 8B) from a computer simulation. The black part of the electrode is electrically insulated, and heating due to RF current results around the exposed metal electrode (electrode tip, shown in gray). Black arrowhead marks boundary of ablation zone (~50 °C).

Current RF ablation devices use either of the following three methods to control applied power:
Power Control: Electrical voltage applied to the RF electrode is adjusted to keep applied RF power constant.

Temperature Control: One or more thermal sensors (either thermocouples or thermistors) are integrated in the RF electrode, typically near the tip. Applied RF power is adjusted to keep the measured temperature at a defined target value.

Impedance Control: RF power is adjusted depending on tissue impedance, which is measured between the RF electrode and the ground pad (see Fig. 1). As tissue vaporizes, an increase in impedance results (details described under “electrical tissue conductivity” further below). When impedance exceeds a certain threshold, RF power is shut down for a certain time period to allow vapor to settle, and then re-applied at a lower level. Figure 4 shows a typical time course of impedance during an impedance-controlled RF ablation.

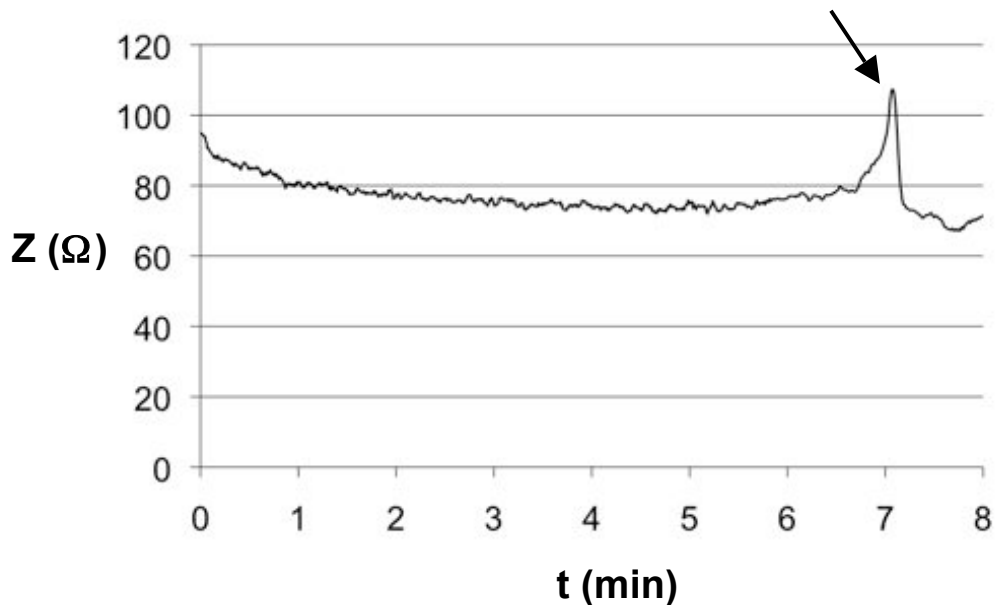


Figure 4. Time course of Impedance (Z) during an impedance-controlled ablation procedure. When impedance exceeds a defined threshold (arrow) as a result of tissue vapor forming around the RF electrode, power is reduced or turned off and re-applied after vapor settles.

II.A. Electrode Cooling

A method that has been employed to RF ablation devices, as well as for other ablative methods (e.g. microwave, laser) to increase the ablation zone is cooling of the RF electrode (or Microwave antenna, Laser fiber). Without electrode cooling, the tissue region of highest temperature is located right next to the electrode (Fig. 5), since that is the location of highest electrical current density (Fig. 6B). By actively cooling the electrode – typically via internal perfusion with water – the tissue in close proximity of the electrode is cooled. This results in the location of highest tissue temperature being moved further into the tissue, producing a larger ablation zone (Fig. 5)¹³. During cardiac ablation procedures, part of the ablation electrode is in contact with the blood pool inside the heart, and convective cooling by the blood passing by the electrode provides a similar effect to active cooling. This is described in more detail below in the section on cardiac RF ablation.

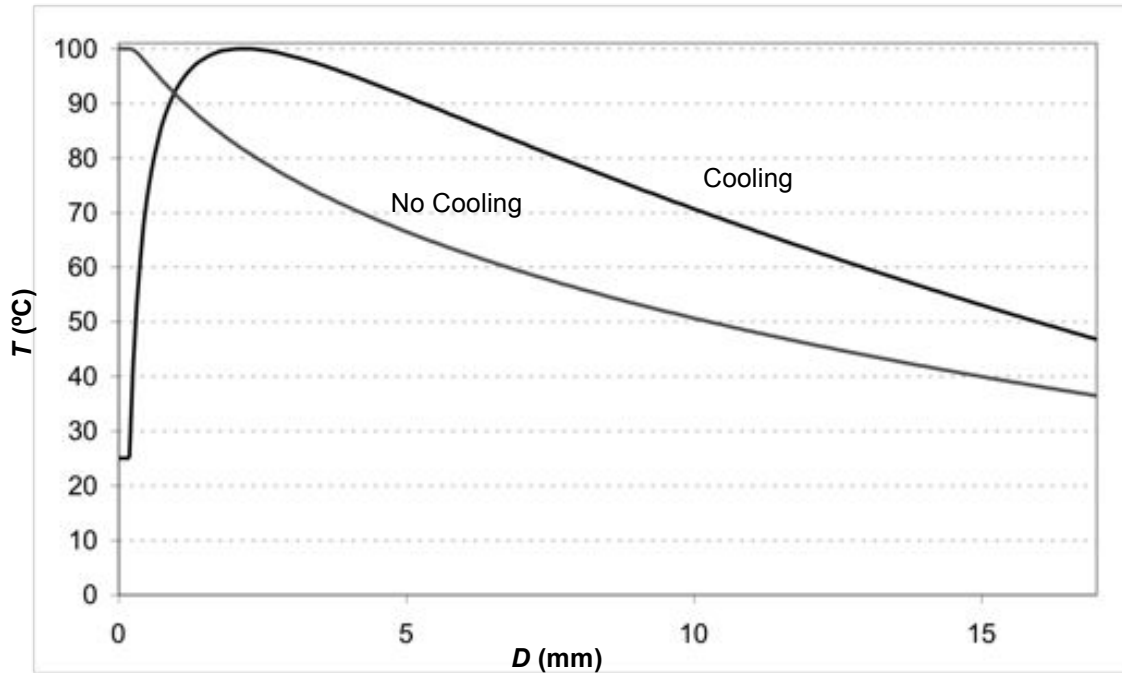


Figure 5. Tissue temperature (T) as a function of distance (D) from the RF electrode. Without cooling, location of maximum tissue temperature is adjacent to the electrode. With cooling, this location is moved further from the electrode, resulting in a larger ablation zone. © 2003, IEEE; Reproduced with permission ¹³.

III. ELECTRICAL TISSUE CONDUCTIVITY

Both thermal and dielectric tissue properties affect tissue temperature during RF ablation. Since thermal properties are discussed in more detail in another paper in this issue by Payne et al., here we will focus on dielectric tissue properties at radiofrequencies. Electrical tissue conductivity is one of the primary parameters that determine current flow through tissue, and local amount of heat generated from RF current (see Equ. 1). In general, electrical tissue conductivity is dependent on frequency with similar behavior to that of a suspension of dielectric particles. The frequency dependence ensues from accumulation of charges (i.e. ions) around the cell membrane (interface polarization) ¹⁴.

Here we will only consider the radiofrequency range, i.e. in the following paragraphs when we refer to electrical conductivity we always assume a frequency around 500 kHz as used during RF ablation. There are a considerable number of studies that measured electrical conductivity (or electrical resistivity, which is the inverse of conductivity) in various tissues at radiofrequencies ¹⁵⁻¹⁸. Note however, that most studies have measured electrical conductivity in ex-vivo tissue; this is important as conductivity changes considerably right after tissue extraction, and continues to change for several hours thereafter ^{19, 20}.

Table I shows electrical conductivity at ~500 kHz for various types of tissues from measurements in animal studies. The low electric conductivity of air inside lung alveoli likely is one of the reasons why RF tumor ablation in lung is less effective, and creates smaller ablation zones than in other tissues ²¹.

TABLE I. Electrical tissue conductivity at a frequency of 500 kHz (=RF ablation frequency)

Tissue Type	Electrical conductivity σ (S/m)	Reference
Normal Liver (rat, in-vivo)	0.36	22
Liver Tumor (rat, in-vivo)	0.45	22
Myocardium (porcine, in-vivo)	0.54	20
Lung inflated (porcine, ex-vivo, 37°C)	0.1	18
Fat (porcine, ex-vivo, 22 °C)	0.02	23
Bone (porcine, ex-vivo, 20 °C)	0.03	18
Blood (rabbit, ex-vivo, 20 °C)	0.7	17
Vaporized Tissue	~1e-15	Assumed same as air

Relevant to RF tumor ablation procedures is, that several studies report differences between normal and tumor tissue electrical conductivity^{22, 24-27}. E.g. an in-vivo animal study in rat tumors found that cancer tissue has about 1.25 times higher electrical conductivity compared to normal tissue. This difference is even more pronounced in lower frequency ranges, and is likely due to loss of membrane integrity associated with cell necrosis often present in tumors²².

Electrical tissue conductivity changes considerably during heating. One component is an increase in conductivity due to higher ion mobility – something that is also observed in ionic solutions, e.g. saline²⁸. In fact, at lower temperature ranges the temperature coefficient of tissue is with 1.5 % similar to that of saline. At higher temperatures (> 50 °C) irreversible changes that affect electrical tissue properties take place. Pop et al. separated reversible and irreversible components in normal kidney tissue and fat at temperatures up to 80 °C, and was able to fit them to an Arrhenius type model²³. The irreversible changes resulted in a permanent increase in electrical conductivity. Similar changes were observed in a recent study performed on surgically removed liver and tumor tissue from metastatic liver cancer patients, where electrical conductivity was measured before and after tissue ablation²⁹. While exact mechanisms that result in irreversible changes are not clear, changes at the cellular level – in particular changes of cell membrane properties – as well as dehydration are likely two important factors.

The initial conductivity increase due to heating results in the early decrease of impedance typically observed during ablation procedures (see Fig. 4). Note that impedance, which is measured between the RF electrode and the reference electrode (i.e. ground pad), represents a weighted average of the electrical resistivity (=1/conductivity) of all tissue that serves as electrical pathway between the two electrodes. The weighting is such that tissue close to the RF electrode has highest influence (i.e. regions with high electric current densities have highest

weighting, see also Fig. 6). Therefore any local changes in electrical conductivity close to the electrode will have most effect on measured impedance.

At high temperatures above ~ 100 °C tissue vaporization takes place; since vapor has a very low electrical conductivity (i.e. is insulating), an increase in impedance is observed (Fig. 4). Figure 6 shows the local changes in electrical current density due to vapor formation, resulting in a drop of current density at locations where vapor forms; i.e. at these locations there is no considerable heating due to RF energy preventing further temperature increases.

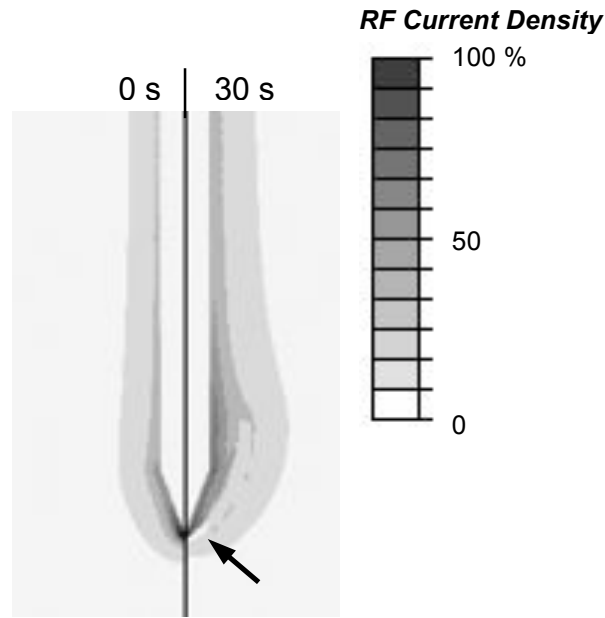


Figure 6. Electrical RF current density for cooled needle electrode at beginning of ablation (left), and after 30 s (right). Due to tissue vaporization around 100 °C and associated drop in local electrical conductivity, current density drops after 30 s around the electrode tip (arrow), since at this location temperatures above 100 °C are obtained first. Current density is shown as percentage of maximum. Reproduced with permission ³⁰.

IV. CLINICAL APPLICATIONS

IV.A. Cancer Treatment

From the early 1990s, RF ablation was started being clinically used for cancer treatment. Initially it was used primarily for liver tumors, since standard treatment options (chemotherapy, radiation therapy) don't work well for liver cancer and most patients are not surgical candidates ³¹. Long term survival data in patients with both primary and metastatic liver cancer suggests that with proper patient selection similar patient survival rates as with surgical tumor removal (the current gold standard) is attainable ^{32, 33}. In recent years the procedure has expanded to other cancer types such as lung, kidney, bone, and adrenal gland ³⁴. Particularly for lung cancer RF ablation has received considerable attention, as there are more than 200,000 new cases of lung cancer reported annually in the US alone ³⁵, and most patients are not surgical candidates; recent studies suggest that patients with inoperable lung cancer may benefit from RF ablation ^{34, 36}. Figure 7 shows an over view of the procedure, where the RF electrode (ablation catheter) is inserted into the liver tumor guided by ultrasound imaging. Typically, contrast enhanced CT or ultrasound is used to guide the procedure; after ablation, the dimensions of the ablation zone

are confirmed with typically contrast-enhanced CT imaging that shows coagulated tissue regions that are devoid of perfusion^{31, 37}. Since several years contrast agents have been available in Europe for ultrasound imaging that allow monitoring of tissue coagulation during the procedure³⁸, but these are not available yet in the United States.

The ablation procedure can be performed minimally invasive through a small incision in the skin (by an interventional radiologist), or during laparoscopy or open surgery (by a surgeon). The patient is typically under light general anesthesia, or under conscious sedation and can leave the hospital the same, or the next day.

The goal is to create an ablation zone that encompasses the tumor as visible under imaging plus a ~1 cm margin of normal tissue to ensure destruction of any cancer microsattelites that often surround the tumor³⁹. For large tumors multiple overlapping ablations created either sequentially⁴⁰, or simultaneously with multiple electrodes⁴¹ are necessary.

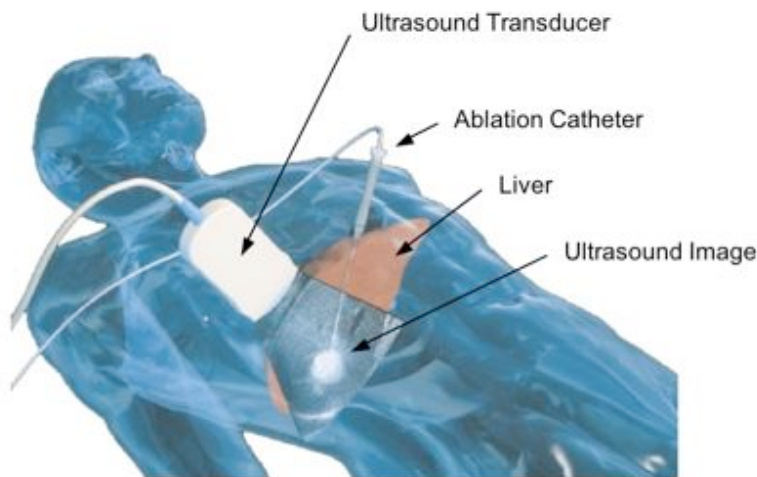


Figure 7. Schematics of minimally-invasive liver tumor RF ablation procedure. The ablation catheter is inserted through a small incision and steered into the tumor under ultrasound imaging guidance. Reproduced with permission⁴².

A number of RF devices for tumor ablation are commercially available. The devices employ different power control algorithms, and different methods to increase the size of the ablation zone. Some devices have multiple tines that are extended from the catheter tip after placement in the tumor (Fig. 8A), others use needle type electrodes with cooling as described earlier (Fig. 8B).

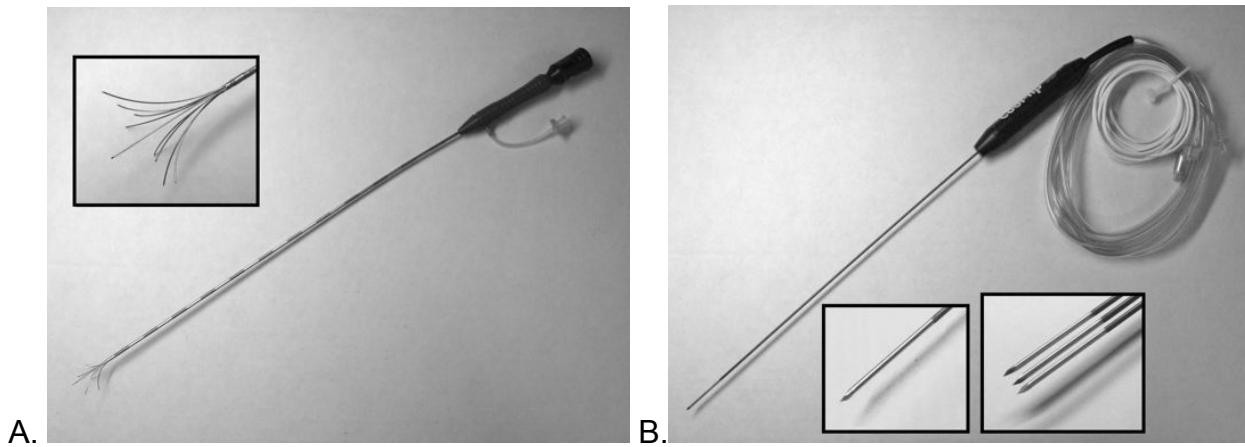


Figure 8. Commercial RF electrodes for tumor ablation. (A) Multi-prong electrode, with magnified electrode tip shown in insert. The prongs are extended once the catheter is placed in the tumor. (B) Cooled needle electrode, available as single, or three-needle cluster (see magnified inserts). Active electrode at the tip is 3 cm (single) or 2.5 cm long (cluster), and is internally cooled by circulating water. Reproduced by permission from Editors (Shahram Vaezy and Vesna Zderic), *Image-guided Therapy Systems*, Norwood, MA: Artech House, Inc., 2009. © 2009 by Artech House, Inc.

Limitation of current RF tumor ablation procedure include: (1) limited performance close to large vasculature, that may result in tumor recurrence due to inadequate temperatures ; (2) inadequate intra-procedural imaging feedback on ablation zone growth; (3) the size of the ablation zone of a single ablation is often not adequate to treat large tumors (> 3 cm diameter), resulting in prolonged procedural times and higher recurrence rates. Current research tries to address these shortcomings, e.g. by:

- Improving efficacy via pre- and intra-operative treatment planning software ⁴³ (see paper by Schumann et al. in this issue)
- Multi-modality image fusion and device tracking ⁴⁴
- Development of new imaging modalities for real-time guidance of the procedure ⁴⁵⁻⁴⁷
- Adjuvant use of chemotherapy or radiation therapy to take advantage of synergy between multiple therapies ⁴⁸⁻⁵⁰

IV.B. Cardiac arrhythmia treatment

RF ablation (a.k.a. cardiac RF catheter ablation) has become the treatment of choice for a number of cardiac arrhythmias (i.e. irregular heart beats), including several types of tachycardia (fast heart rhythm above 150 bpm), and more recently atrial fibrillation (i.e. quivering of the atria) ^{1, 51}. Cardiac arrhythmias result from abnormalities in the cardiac conduction system, which determines the spatial and temporal activation of different parts of the heart.

Cardiac ablation is performed by an electrophysiologist in a specifically equipped interventional laboratory, where a catheter is inserted into a vein (typically in the groin or neck) and steered into the heart (Fig. 9). The procedure is guided by X-ray imaging, and by electrical measurements of local cardiac activity (similar to ECG) by the RF catheter (Fig. 10), as well as

by additional specialized recording catheters placed at various locations in the heart. These local electrical activity measurements allow determination of when different parts of the heart are activated, and thereby facilitate accurate diagnosis of the arrhythmia as well as localization of the exact target site. For complex arrhythmia types, computer assisted diagnostic systems are available that use electromagnetic tracking of a special catheter and correlate recordings of this catheter at various locations to produce so-called “activation maps” that depict the spread of activation through the heart. Other systems use measurements of tissue impedance between a catheter electrode and a set of reference electrodes, or systems based on ultrasound propagation timing to localize the catheter position⁵².

After the RF catheter is steered to the target site, RF current is applied and produces a small ablation zone around the active electrode tip. A single application last typically 45 – 120 s, and produces an ablation zone ~5 – 10 mm diameter (Figs. 11, 12).

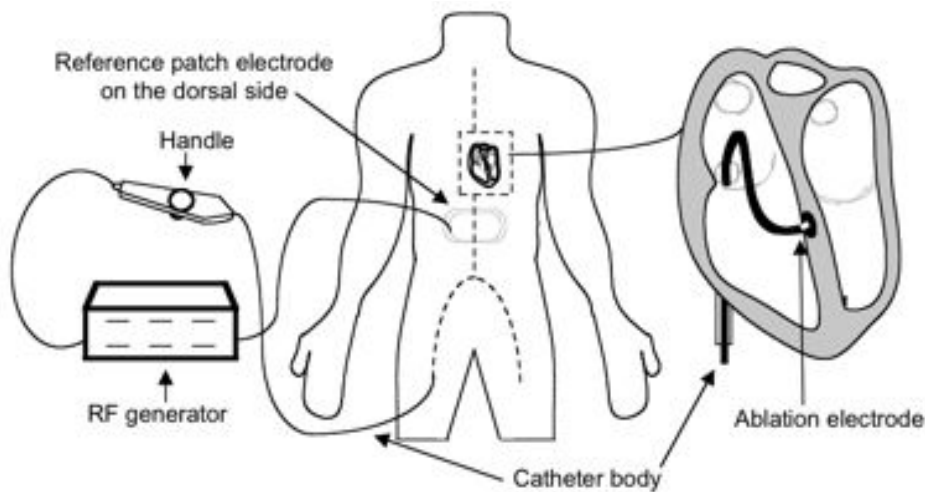


Figure 9. Schematics of cardiac RF ablation system. A cardiac RF catheter is inserted through a leg vein, and steered to the target site inside the heart (right figure). A reference patch electrode (i.e. ground pad) is placed on the patient’s back. The small black region around the RF electrode at the catheter tip depicts the ablation zone. © 1995, IEEE; Reproduced with permission⁵³.

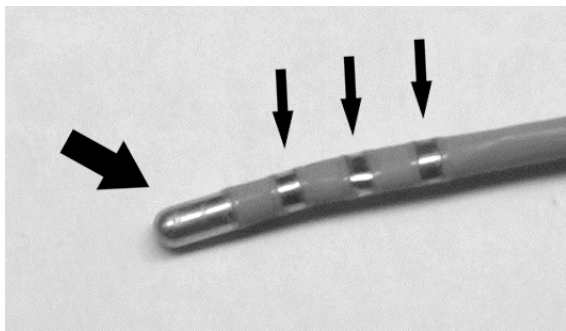


Figure 10. Cardiac RF ablation catheter (7F = 2.3 mm diameter). Catheter has an RF electrode (large arrow, 4 mm length) to create the ablation zone, and mapping electrodes (small arrows) to record electrical activity from within the heart. Reproduced by permission from Editors (Shahram Vaezy and Vesna Zderic), *Image-guided Therapy Systems*, Norwood, MA: Artech House, Inc., 2009. © 2009 by Artech House, Inc.

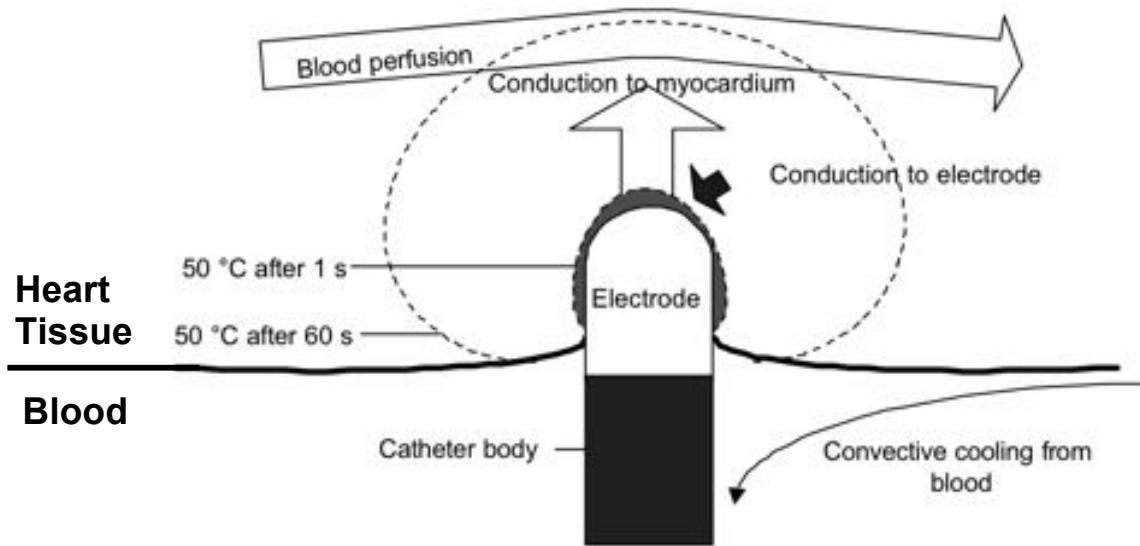


Figure 11. Thermodynamics of cardiac RF ablation: RF electrode is in contact with myocardium (heart tissue), and RF current results in tissue heating. Thermal conduction of heat into the tissue results in growth of the ablation zone (approximated by 50°C-isotherm). Heat loss of tissue in proximity of the electrode due to thermal conduction through the electrode (black arrow); electrode and tissue surface experience convective cooling from blood inside the chamber. Surface cooling produces the typical tear drop shaped ablation zone (reproduced from Tungjtkusolmun⁵⁴)

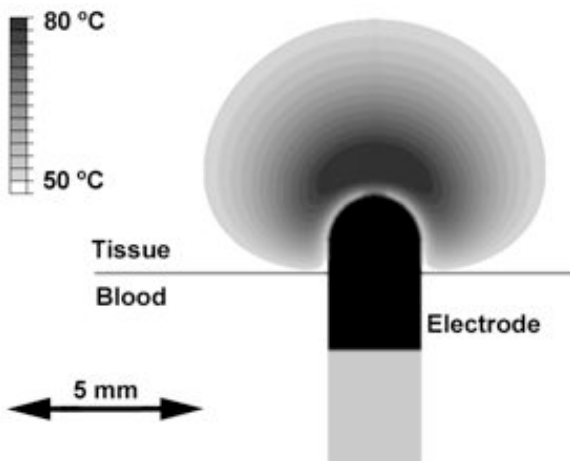


Figure 12. Tissue temperature around a cardiac RF ablation catheter (2.3 mm diameter) at the end of a 45 s ablation. Outermost 50°C- boundary estimates boundary of ablation zone. Reproduced by permission from Editors (Shahram Vaezy and Vesna Zderic), *Image-guided Therapy Systems*, Norwood, MA: Artech House, Inc., 2009. © 2009 by Artech House, Inc.

Most catheters employ temperature control, where temperature measured within the electrode tip is used to adjust applied RF energy. Note however that the location of maximum tissue temperature is a few mm from the catheter tip (Fig. 11), i.e. that the measured temperature underestimates maximum tissue temperature depending on local blood flow conditions. This is particularly important since undesired tissue perforation (often called ‘popping’ due to the sound associated with this event) can occur when tissue vaporized above 100 °C. Popping is often associated with an impedance spike similar to the one shown in Fig. 3. As noted, intra-cardiac blood flow considerably affects tissue heating, and resulting size of the ablation zone. In general, larger ablation zones are possible at locations with high flow-rate due to increased convective cooling (see Fig. 5)⁵⁵⁻⁵⁷. Catheters of different lengths and diameters are commercially available depending on desired size of the ablation zone. Newer catheter designs employ internal cooling to increase ablation zone size.

Atrial Fibrillation (where the atria quiver instead of beating reducing pumping performance of the heart, and with risk of blood clot formation) is a common arrhythmia type affecting ~2.2 million people in the US, and is particularly prevalent in people older than 60 years⁵¹. Cardiac ablation is increasingly used for treatment of atrial fibrillation if the patient does not respond to medication. Successful treatment via ablation requires creating multiple linear, contiguous ablation zones. This is difficult and time consuming with current devices, resulting in long procedural times and high recurrence rates⁵¹. New devices that allow more rapid and reliable creation of linear ablation zones are in development^{58, 59}.

IV.C. Other applications

RF ablation is clinically used for treatment of uterine bleeding in women that don’t respond to standard treatments such as drugs and scraping of the endometrium. During treatment, the whole endometrium (i.e. lining of the uterus) is ablated within typically 3 – 10 minutes. While most devices use heated aqueous solutions to ablate the tissue, there is also a RF based device available that employs mesh electrodes with power applied between two meshes in bipolar fashion⁴.

Endovascular ablation is a treatment modality for varicose veins, i.e. visible, dilated and twisted veins near the skin surface. Varicose veins most often affect legs and thighs, where insufficiencies in the venous valves result in blood pooling and vein enlargement. Treatment options aim to close the affected veins and include surgical stripping, injection of a drug that results in vein swelling and closure, and ablation. During ablation, a catheter is introduced into the vein, and the vessel wall is heated resulting in collagen shrinkage and closure of the vein. Laser- and RF-based endovascular ablation devices are commercially available⁵.

V. CONCLUSIONS

RF ablation allows localized tissue destruction via heating, and has as such found clinical application in several diseases where a specified region of tissue needs to be destroyed. Image guidance for RF ablation procedures is in general of great importance as it allows identification and visualization of the target region, and guidance of the procedure. Improvement of imaging modalities in the near future will allow for improved accuracy of RF ablation and thermal therapies in general. Real-time feedback on size of the growing ablation zone during treatment is currently limited, and this is another area where improved imaging could have great impact. Thermal therapies such as RF ablation will likely play a considerable role in patient treatment in the foreseeable future, and one major area of continued growth is likely for cancer treatment where there is a need for therapies that can accurately produce localized tissue destruction.

REFERENCES

1. Huang S, Wood M. Catheter Ablation of Cardiac Arrhythmias: Saunders, 2006.
2. vanSonnenberg E. Tumor ablation. 1st ed. New York, NY: Springer, 2005.
3. Haemmerich D. Tissue Ablation. In Webster JG, ed. Wiley Encyclopedia of Medical Devices and Instrumentation, Vol. 6. New Jersey: John Wiley & Sons, 2006. pp. 362 - 379.
4. Cooper J, Gimpelson RJ. Summary of safety and effectiveness data from FDA: a valuable source of information on the performance of global endometrial ablation devices. *J Reprod Med* 2004; 49(4):267-73.
5. Markovic JN, Shortell CK. Update on radiofrequency ablation. *Perspect Vasc Surg Endovasc Ther* 2009; 21(2):82-90.
6. Steinke K, Gananadha S, King J, Zhao J, Morris DL. Dispersive pad site burns with modern radiofrequency ablation equipment. *Surg Laparosc Endosc Percutan Tech* 2003; 13(6):366-71.
7. Schramm W, Yang D, Wood BJ, Rattay F, Haemmerich D. Contribution of direct heating, thermal conduction and perfusion during radiofrequency and microwave ablation. *Open Biomedical Engineering Journal* 2007; 1):47-52.
8. Diller KR, Valvano JW, Pearce JA. Bioheat Transfer. In Kreith F, ed. *CRC Handbook of Thermal Engineering*, Vol. 4. Boca Raton: CRC Press, 2000. pp. 114 - 215.
9. Arkin H, Xu LX, Holmes KR. Recent developments in modeling heat transfer in blood perfused tissues. *IEEE Trans. Biomed. Eng.* 1994; 41(2):97-107.
10. Pennes HH. Analysis of tissue and arterial blood temperatures in the resting human forearm. *J. Appl. Physiol.* 1948; 1(2):93-122.
11. Dewhirst MW, Viglianti BL, Lora-Michiels M, Hanson M, Hoopes PJ. Basic principles of thermal dosimetry and thermal thresholds for tissue damage from hyperthermia. *Int J Hyperthermia* 2003; 19(3):267-94.
12. Berjano EJ. Theoretical modeling for radiofrequency ablation: state-of-the-art and challenges for the future. *Biomed Eng Online* 2006; 5):24.
13. Haemmerich D, Chachati L, Wright AS, Mahvi DM, Lee FT, Jr., Webster JG. Hepatic radiofrequency ablation with internally cooled probes: effect of coolant temperature on lesion size. *IEEE Transactions on Biomedical Engineering* 2003; 50(4):493-500.
14. Pethig R, Kell DB. The passive electrical properties of biological systems: their significance in physiology, biophysics and biotechnology. *Phys Med Biol* 1987; 32(8):933-70.
15. Duck FA. Chapter 6: Electrical Properties of Tissue. *Physical Properties of Tissue*. London: Academic Press, 1990. pp. 167-223.
16. Foster KR, Schwan HP. Dielectric properties of tissues and biological materials: a critical review. *Crit Rev Biomed Eng* 1989; 17(1):25-104.
17. Gabriel C, Gabriel S, Corthout E. The dielectric properties of biological tissues: I. Literature survey. *Physics in Medicine and Biology* 1996; 41(11):2231-2249.
18. Gabriel S, Lau RW, Gabriel C. The dielectric properties of biological tissues: II. Measurements in the frequency range 10 Hz to 20 GHz. *Physics in Medicine and Biology* 1996; 41(11):2251-2269.
19. Haemmerich D, Ozkan OR, Tsai JZ, Staelin ST, Tungjitkusolmun S, Mahvi DM, Webster JG. Changes in electrical resistivity of swine liver after occlusion and postmortem. *Medical and Biological Engineering and Computing* 2002; 40(1):29-33.
20. Tsai JZ, Will JA, Hubbard-Van Stelle S, Cao H, Tungjitkusolmun S, Choy YB, Haemmerich D, Vorperian VR, Webster JG. In-vivo measurement of swine myocardial resistivity. *IEEE Trans Biomed Eng* 2002; 49(5):472-483.
21. Brace CL. Radiofrequency and microwave ablation of the liver, lung, kidney, and bone: what are the differences? *Curr Probl Diagn Radiol* 2009; 38(3):135-43.
22. Haemmerich D, Staelin ST, Tungjitkusolmun S, Mahvi DM, Webster JG. In-vivo conductivity of hepatic tumors. *Physiological Measurement* 2003; 24(2):251-260.
23. Pop M, Molckovsky A, Chin L, Kolios MC, Jewett MA, Sherar MD. Changes in dielectric properties at 460 kHz of kidney and fat during heating: importance for radio-frequency thermal therapy. *Phys Med Biol* 2003; 48(15):2509-25.
24. Esrick MA, McRae DA. The effect of hyperthermia-induced tissue conductivity changes on electrical impedance temperature mapping. *Phys Med Biol* 1994; 39(1):133-44.
25. Lu Y, Li B, Xu J, Yu J. Dielectric properties of human glioma and surrounding tissue. *Int J Hyperthermia* 1992; 8(6):755-60.
26. Surowiec AJ, Stuchly SS, Barr JB, Swarup A. Dielectric properties of breast carcinoma and the surrounding tissues. *IEEE Trans Biomed Eng* 1988; 35(4):257-63.

27. Swarup A, Stuchly SS, Surowiec A. Dielectric properties of mouse MCA1 fibrosarcoma at different stages of development. *Bioelectromagnetics* 1991; 12(1):1-8.
28. Stogryn A. Equations for calculating the dielectric constant of saline water. *IEEE Transactions on Microwave Theory and Techniques* 1971; 19):733-736.
29. Haemmerich D, Schutt DJ, Wright AW, Webster JG, Mahvi DM. Electrical conductivity measurement of excised human metastatic liver tumours before and after thermal ablation. *Physiol Meas* 2009; 30(5):459-466.
30. Haemmerich D, Wood BJ. Hepatic radiofrequency ablation at low frequencies preferentially heats tumour tissue. *Int J Hyperthermia* 2006; 22(7):563-74.
31. Rhim H, Dodd GD, 3rd. Radiofrequency thermal ablation of liver tumors. *J Clin Ultrasound* 1999; 27(5):221-9.
32. Gillams AR, Lees WR. Five-year survival in 309 patients with colorectal liver metastases treated with radiofrequency ablation. *Eur Radiol* 2009; 19(5):1206-13.
33. Livraghi T, Meloni F, Di Stasi M, Rolle E, Solbiati L, Tinelli C, Rossi S. Sustained complete response and complications rates after radiofrequency ablation of very early hepatocellular carcinoma in cirrhosis: Is resection still the treatment of choice? *Hepatology* 2008; 47(1):82-9.
34. Gillams A. Tumour ablation: current role in the liver, kidney, lung and bone. *Cancer Imaging* 2008; 8 Suppl A):S1-5.
35. Jemal A, Siegel R, Ward E, Murray T, Xu J, Thun MJ. Cancer statistics, 2007. *CA Cancer J Clin* 2007; 57(1):43-66.
36. Simon CJ, Dupuy DE, DiPetrillo TA, Safran HP, Grieco CA, Ng T, Mayo-Smith WW. Pulmonary radiofrequency ablation: long-term safety and efficacy in 153 patients. *Radiology* 2007; 243(1):268-75.
37. Raman SS, Lu DS, Vodopich DJ, Sayre J, Lassman C. Creation of radiofrequency lesions in a porcine model: correlation with sonography, CT, and histopathology. *American Journal of Roentgenology* 2000; 175(5):1253-1258.
38. Solbiati L, Ierace T, Tonolini M, Cova L. Guidance and monitoring of radiofrequency liver tumor ablation with contrast-enhanced ultrasound. *Eur J Radiol* 2004; 51 Suppl):S19-23.
39. Sasaki A, Kai S, Iwashita Y, Hirano S, Ohta M, Kitano S. Microsatellite distribution and indication for locoregional therapy in small hepatocellular carcinoma. *Cancer* 2005; 103(2):299-306.
40. Chen MH, Yang W, Yan K, Zou MW, Solbiati L, Liu JB, Dai Y. Large liver tumors: protocol for radiofrequency ablation and its clinical application in 110 patients--mathematic model, overlapping mode, and electrode placement process. *Radiology* 2004; 232(1):260-71.
41. Laeseke PF, Frey TM, Brace CL, Sampson LA, Winter TC, 3rd, Ketzler JR, Lee FT, Jr. Multiple-electrode radiofrequency ablation of hepatic malignancies: initial clinical experience. *AJR Am J Roentgenol* 2007; 188(6):1485-94.
42. Dodd GD, Soulen MC, Kane RA, Livraghi T, Lees WR, Yamashita Y, Gillams AR, Karahan OI, Rhim H. Minimally invasive treatment of malignant hepatic tumors: At the threshold of a major breakthrough. *Radiographics* 2000; 20(1):9-27.
43. Weihusen A, Ritter F, Kroger T, Preusser T, Zidowitz S, Peitgen H-O. Workflow oriented software support for image guided radiofrequency ablation of focal liver malignancies. In Kevin RC, Michael IM, eds., Vol. 6509: SPIE, 2007. pp. 650919.
44. Wood BJ, Locklin JK, Viswanathan A, Kruecker J, Haemmerich D, Cebal J, Sofer A, Cheng R, McCreedy E, Cleary K, McAuliffe MJ, Glossop N, Yanof J. Technologies for guidance of radiofrequency ablation in the multimodality interventional suite of the future. *J Vasc Interv Radiol* 2007; 18(1 Pt 1):9-24.
45. Bharat S, Fisher TG, Varghese T, Hall TJ, Jiang J, Madsen EL, Zagzebski JA, Lee FT, Jr. Three-dimensional electrode displacement elastography using the Siemens C7F2 fourSight four-dimensional ultrasound transducer. *Ultrasound Med Biol* 2008; 34(8):1307-16.
46. Daniels MJ, Varghese T, Madsen EL, Zagzebski JA. Non-invasive ultrasound-based temperature imaging for monitoring radiofrequency heating-phantom results. *Phys Med Biol* 2007; 52(16):4827-43.
47. Brace CL, Mistretta CA, Hinshaw J, Lee FT. Periodic contrast-enhanced computed tomography for thermal ablation monitoring: A feasibility study. *Conf Proc IEEE Eng Med Biol Soc* 2009; 1):4299-302.
48. Martin RC, 2nd, Scoggins CR, McMasters KM. A phase II study of radiofrequency ablation of unresectable metastatic colorectal cancer with hepatic arterial infusion pump chemotherapy. *J Surg Oncol* 2006; 93(5):387-93.
49. Elias D, Baton O, Sideris L, Boige V, Malka D, Liberale G, Pocard M, Lasser P. Hepatectomy plus intraoperative radiofrequency ablation and chemotherapy to treat technically unresectable multiple colorectal liver metastases. *J Surg Oncol* 2005; 90(1):36-42.

50. Solazzo S, Mertyna P, Peddi H, Ahmed M, Horkan C, Goldberg SN. RF ablation with adjuvant therapy: comparison of external beam radiation and liposomal doxorubicin on ablation efficacy in an animal tumor model. *Int J Hyperthermia* 2008; 24(7):560-7.
51. Wilber DJ, Packer DL, Stevenson WG. *Catheter Ablation of Cardiac Arrhythmias: Basic Concepts and Clinical Applications*. Malden, MA: Blackwell Publishing, 2007.
52. Markowitz SM, Lerman BB. How to interpret electroanatomic maps. *Heart Rhythm* 2006; 3(2):240-6.
53. Panescu D, Wayne JG, Fleischman SD, Mirotznik MS, Swanson DK, Webster JG. Three-dimensional finite element analysis of current density and temperature distributions during radio-frequency ablation. *IEEE Transactions on Biomedical Engineering* 1995; 42(9):879-890.
54. Tungjtkusolmun S. *Finite Element Modeling of Radiofrequency Cardiac and Hepatic Ablation*. Biomedical Engineering, Vol. Ph.D. Madison: University of Wisconsin, 2000.
55. Cao H, Vorperian VR, Tungjtkusolmun S, Tsai JZ, Haemmerich D, Choy YB, Webster JG. Flow effect on lesion formation in RF cardiac catheter ablation. *IEEE Trans Biomed Eng* 2001; 48(4):425-33.
56. Tungjtkusolmun S, Vorperian VR, Bhavaraju N, Cao H, Tsai JZ, Webster JG. Guidelines for predicting lesion size at common endocardial locations during radio-frequency ablation. *IEEE Trans Biomed Eng* 2001; 48(2):194-201.
57. Petersen HH, Chen X, Pietersen A, Svendsen JH, Haunso S. Lesion dimensions during temperature-controlled radiofrequency catheter ablation of left ventricular porcine myocardium: impact of ablation site, electrode size, and convective cooling. *Circulation* 1999; 99(2):319-25.
58. Burkhardt JD, Natale A. New technologies in atrial fibrillation ablation. *Circulation* 2009; 120(15):1533-41.
59. Siklody CH, Minners J, Allgeier M, Allgeier HJ, Jander N, Keyl C, Weber R, Schiebeling-Romer J, Kalusche D, Arentz T. Pressure-Guided Cryoballoon Isolation of the Pulmonary Veins for the Treatment of Paroxysmal Atrial Fibrillation. *J Cardiovasc Electrophysiol* 2009.